Limits to Transits of the Neptune-Mass Planet Orbiting GJ 581[1]

Mercedes López-Morales,[2,3,4] Nidia I. Morrell,[5] R. Paul Butler,[2] and Sara Seager[2]
Received 2006 July 18; accepted 2006 September 5; published 2006 November 14

ABSTRACT. We have monitored the Neptune-mass, exoplanet-hosting M dwarf GJ 581 with the 1 m Swope Telescope at Las Campanas Observatory over two predicted transit epochs. A neutral density filter centered at 550 nm was used during the first epoch, yielding 6.33 hr of continuous light-curve coverage with an average photometric precision of 1.6 mmag and a cadence of 2.85 minutes. The second epoch was monitored in the *B* band over 5.85 hr, with an average photometric precision of 1.2 mmag and a 4.28 minute cadence. No transits are apparent on either night, indicating that the orbital inclination is less than 88°.1 for all planets with radii larger than $0.38R_{\rm Nep}$ ($=1.48\ R_{\oplus}$). Because planets with the most likely interior compositions will have radii larger than $1.55\ R_{\oplus}$, we place an inclination limit of 88°.1 for the system. The corresponding minimum mass of the exoplanet GJ 581b remains $0.97M_{\rm Nep}$ ($=16.6\ R_{\oplus}$).

Online material: extended table

1. INTRODUCTION

Bonfils et al. (2005) recently reported the detection of a Neptune-mass planet around the M dwarf GJ 581. This planet, GJ 581b, which has an orbital period of 5.366 days and minimum mass $M_2 \sin i = 0.97M_{\rm Nep}$, is only the fifth one found around M dwarfs. The two other M dwarfs currently known to host planets are GJ 876, with two Jupiter-mass planets (Delfosse et al. 1998; Marcy et al. 1998) and one Neptune-mass planet (Rivera et al. 2005), and GJ 436, with one Neptune-mass planet (Butler et al. 2004). Therefore, GJ 581b is only the third in the class of Neptune-mass planets to be found around an M dwarf.

Of the three Neptune-mass planets, GJ 876d and GJ 436b have been photometrically searched for possible transits (Rivera et al. 2005; Butler et al. 2004), although none have been found. GJ 581b, on the other hand, has not yet been searched for transits. The probability of detecting a transit for GJ 581b is only 3.3%, assuming a stellar radius of $0.29\ R_{\odot}$ and an orbital separation of 0.041 AU (Bonfils et al. 2005). However, if a transit were to occur, the planet would cover a larger fraction of the M dwarf than in the equivalent case of a planet orbiting a Sun-like star. Therefore, transits of GJ 581b would in prin-

ciple be deeper and easier to detect. The detection of a transit would allow us to establish the absolute mass of the planet and its radius. From these parameters, we could also determine the mean density of the planet and estimate its chemical composition.

GJ 581 (V* HO Lib) is an M3 V star that has been cataloged as a BY Draconis variable. This type of variable is characterized by quasi-periodic photometric variations over timescales of less than a day to months, and amplitudes ranging from a few hundredths of a magnitude to 0.5 mag. This variability is generally attributed to surface spots and chromospheric activity, phenomena that are very common among M-type dwarfs. Weis (1994) monitored GJ 581 over 8 years and found seasonal and long-term photometric variations of 6–8 mmag in the *V*, *R*, and *I* bands. However, no measurements of short-term variability (in the scale of hours) have been reported so far. Furthermore, no information is available about the photometric precision of the star at wavelengths bluer than *V*.

This paper presents the first short-term precision light curves of GJ 581 over two predicted planetary transit epochs. The light curves were collected in optical and *B* bands and span 6.33 and 5.85 consecutive hours, respectively. Section 2 describes the observations, with their analysis presented in § 3. The results of a geometric search for transits are presented in § 4.

2. OBSERVATIONS

We measured the light curves between 2:11 and 8:31 UT on 2006 April 24 and 2:22 and 8:44 UT on 2006 May 10 at the Henrietta Swope Telescope, located at Las Campanas Observatory in Chile. Transits were predicted to occur around 2:54 UT on April 24 and 5:16 UT on May 10 (midtransit times), based on the ephemeris given by Bonfils et al. (2005). The

[2] Department of Terrestrial Magnetism, Carnegie Institution of Washington, 5241 Broad Branch Road NW, Washington, DC 20015; mercedes@dtm.ciw.edu, paul@dtm.ciw.edu, seager@dtm.ciw.edu.

[3] Carnegie Fellow.

[4] American Philosophical Society's Lewis and Clark Field Scholar in Astrobiology.

[5] Las Campanas Observatory, Observatories of the Carnegie Institution of Washington, Casilla 601, La Serena, Chile; nmorrell@lco.cl.

estimated minimum duration of the transits is ∼85 minutes, and the uncertainty on the estimated midtransit times is ∼86.4 minutes.

The Swope Telescope is currently equipped with a 2048 × 3150, 15 μm pixel SITe CCD that provides a field of view of 14.8 × 22.8. The dynamic range of the CCD is 32,727 ADU (analog-to-digital converter units), with a gain of 2.5 e^- ADU^{-1}. We used a 2048 × 2048 (14.8 × 14.8) subraster of the CCD to reduce the readout time to 128 s (1 × 1 binning) and therefore increase the duty cycle of our observations. The aperture stop used to avoid saturation of bright stars (as described in López-Morales 2006) has now been replaced by a 10% transmission neutral density filter (ND0.9) with a 3000 Å FWHM passband centered at 5500 Å. We have also added to the setup a standard Johnson B-band filter.

GJ 581 ($V = 10.56$, $B - V = 1.61$) was strategically placed on the CCD so that it included a suitable comparison star in the frames. As as comparison, we used the nearby star BD −06 4172 ($V = 10.50$, $B - V = 1.30$), located at a distance of $\Delta\alpha = 53.76$ and $\Delta\delta = 12.747$ from GJ 581. As a check star, we used a slightly fainter object ($V = 12.2$) located at $\alpha = 15^h19^m27.5$, $\delta = -07°31'44''$ (J2000.0).

All the images from the first night were taken through the neutral density filter ND0.9. We collected a total of 133 images with 30 s exposure times, covering a range of air masses between 1.08 and 1.82. GJ 581 was monitored over 6.33 hr, with an average cadence time of 2.85 minutes. The images on the second night were collected using the B-band filter. A total of 82 images were collected in this case, with exposure times of 120 s and air masses between 1.08 and 1.62. This time we monitored the target over 5.85 hr, with an average cadence time of 4.28 minutes. The photometric precision per frame is ∼3 × 10^{-4} mmag from Poisson noise alone. Equation (10) of Dravins et al. (1998) gives a scintillation level of 0.74 mmag in the ND0.9 band and 0.37 mmag in the B band for our exposure times and an intermediate air mass of 1.4 (for these calculations, we used a telescope aperture diameter of 100 cm, an observatory height of 2100 m, and an atmospheric scale height of 8000 m). Our photometric precision is therefore limited by scintillation.

3. ANALYSIS

Each image was bias subtracted and flat-fielded using the same combined bias and the combined flats in each filter. Next, we performed aperture photometry on the target, comparison, and check stars in each calibrated frame over a series of apertures ranging from between 10 and 30 pixels for the ND0.9 data and between 10 and 26 pixels for the B-band data. The area used to compute the sky background around each star was the same in all frames (i.e., a 15 pixel annulus at a radius of 40 pixels from the center of the stars). The sky background around each star was computed using a σ-clipping algorithm in order to avoid contamination by nearby objects or residual bad pixels. The optimal combination of apertures for each light curve was derived following a procedure that is analogous to the one described in López-Morales (2006).

The average dispersion of the comparison and check stars is of the order of 0.8 mmag in both filters. Small differential extinction effects are apparent in the differential light curve of the target and comparison stars. Those effects have been corrected by applying second-order extinction correction equations, of the form

$$\Delta\text{ND} = \Delta nd - k_{nd}\Delta X + c_{nd}\Delta(B - V) \tag{1}$$

and

$$\Delta B = \Delta b - k_b\Delta X + c_b\Delta(B - V), \tag{2}$$

where Δ indicates the difference in the associated quantities for each star, as derived by Hardie (1962), Δnd and Δb are the differences in instrumental magnitude of the target and comparison stars in ND0.9 and the B band, respectively, and ΔX is the difference in air mass between the two objects. This value changes with time, depending on the position of the objects in the sky. In our particular case, the absolute value of ΔX varies between 1.5×10^{-4} and 1.3×10^{-2} for the range of air mass covered by our observations. The expression $\Delta(B - V)$ is the difference in color between the two stars; in this case $\Delta(B - V) = 0.3$. Finally, (k_{nd}, c_{nd}) and (k_b, c_b) denote the extinction and color coefficients in ND0.9 and B, respectively. The values of these coefficients have been adopted from recent measurements by Hamuy et al. (2006), who computed average values of extinction and color coefficients at the Swope Telescope over ∼230 nights and in different filter bands. For the ND0.9 filter, we used the values of the coefficients in the V band.

The final light curves are presented in Figure 1: panel a shows the 6.33 hr time series coverage of GJ 581 with the ND0.9 filter, with an average standard deviation of the light curve of 1.65 mmag, and panel b shows the B-band light curve, with a time coverage of 5.85 hr. The average standard deviation of the light curve in this case is 1.17 mmag. A file containing the data in this figure is available online, a sample of which is illustrated in Table 1. Note that the observed photometric dispersion in the light curves is larger than expected from the scintillation levels computed in § 2. This discrepancy can be attributed to uncertainties in the estimation of scintillation noise, low-level systematics in our data, or the intrinsic variability of the stars.

4. SEARCH FOR TRANSITS

To determine whether or not a planet transit is present in our data, we need to estimate the duration and depth of the GJ 581b transit. In turn, we need to estimate the radii of the planet and the star, the orbital separation between the two objects, and the orbital period of the system.
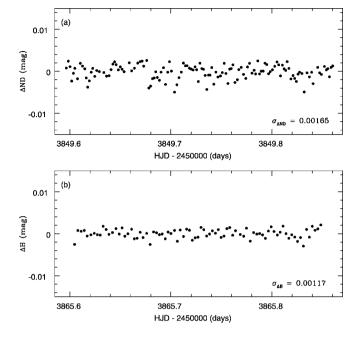
FIG. 1.—Light curves of GJ 581 with (*a*) the ND0.9 filter and (*b*) the *B*-band filter. The time coverage in (*a*) is 6.33 hr, with an average photometric dispersion of 1.65 mmag. The time coverage in (*b*) is 5.85 hr, with an average photometric dispersion of 1.17 mmag.

The orbital separation and period have been determined by Bonfils et al. (2005), who find GJ 581b to be on a circular orbit around the star, at a distance of 0.041 AU and with an orbital period of 5.366 days. GJ 581 is an M3 dwarf with an estimated mass of $0.31 \pm 0.02 \ M_{\odot}$ (estimated from stellar mass–luminosity relations; see Bonfils et al. 2005). This mass corresponds to a radius of about $0.29 \pm 0.03 \ R_{\odot}$, based on mass-radius relation models by Baraffe et al. (1998).

The radius of the planet will depend heavily on its interior chemical composition. A Neptune-mass planet can plausibly range from 1.55 to 9.5 $R_{\oplus}$, depending on whether the object is entirely composed of iron (Seager et al. 2006, in preparation) or if it is an evaporating H/He gas planet (Baraffe et al. 2005). The radius of a planet composed of a large fraction of H/He and as close to the host star as GJ 581b will also be affected by the amount of stellar luminosity incident on the planet. This in turn depends on the distance to the star, as well as the planet's albedo and energy transportation mechanism. These last two parameters are currently unknown for extrasolar planets. At present, only an estimation of the albedo of HD 209458b has been reported by Rowe et al. (2006), who find a 3 σ upper limit of ~0.25 for this parameter. For all of the above reasons, it is difficult to estimate a radius for GJ 581b in the absence of any measured transits.

Based on geometry alone, we can estimate upper limits for the transit depth and hence planet radius. Assuming an edge-on configuration ($i = 90°$) and a circular orbit, the transit can

TABLE 1
B-BAND LIGHT-CURVE DATA USED IN FIG. 1

HJD (days)	ΔB (mag)	$\sigma_{\Delta B}$ (mag)
2,453,865.604493	−0.0025374	0.0000005
2,453,865.607757	0.0007653	0.0000005
2,453,865.611091	0.0005909	0.0000005
2,453,865.614100	0.0007751	0.0000005
2,453,865.616947	−0.0005518	0.0000005

NOTE.—Table 1 is published in its entirety in the electronic edition of the *PASP*. A portion is shown here for guidance regarding its form and content.

last between 85 and 99 minutes for a range of planetary radii of 1.48–7 $R_{\oplus}$. This range of radii also gives transit depths of between ~2.5 and 54 mmag, assuming full transits and a uniform luminosity of the surface of the star (i.e., no limb darkening or star spots).

Figure 2 shows a schematic of full transits of a 1.48 $R_{\oplus}$ (*solid line*), 3.9 $R_{\oplus}$ (*dashed line*), and 7.0 $R_{\oplus}$ (*dotted line*) planet superimposed on our ND0.9 filter and *B*-band light curves. These schematic box models do not include any physical effects associated with either the planet or the star. The horizontal error bars below each transit illustrate the uncertainty in the predicted midtransit time. The 2 σ limit in the photometric dispersion of the light curves around the expected time of transit
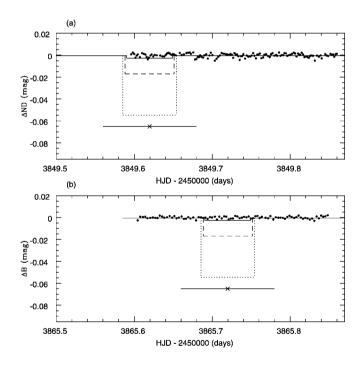

FIG. 2.—Schematic representation of geometric transits for three possible values of the planet's radius—1.48 $R_{\oplus}$ (*solid line*), 3.9 $R_{\oplus}$ (*dashed line*), and 7.0 $R_{\oplus}$ (*dotted line*)—overplotted on (*a*) our ND0.9 filter and (*b*) *B*-band filter light curves. The solid lines under each transit illustrate the uncertainty in the predicted times of eclipse (86.4 minutes), with the predicted midtransit times marked as crosses.

(binned in a 85 minute time bin) is ~2 mmag in both light curves.

It is clear that transits at the illustrated depths and durations do not occur during either one of the predicted transit windows. From the $2\,\sigma$ limit above, combined with the radius for GJ 876, we can dismiss the presence of full transits of planets as small as $1.48\,R_\oplus$ at inclinations higher than $88°\!.1$.

Our observations therefore rule out transits of GJ 581b for inclinations larger than $88°\!.1$ and planetary radii larger than $1.48\,R_\oplus$. Transits could still be present if $R_p < 1.48\,R_\oplus$, because they are not detectable within the photometric dispersion of our light curves. Only higher precision ground- or space-based observations will be able to find out if transits of planets smaller than our radius detection limit occur. Intrinsic low-amplitude photometric variability of the star will most likely impose the final limit to detectable transit depths. However, we do note that the star appears to be more photometrically stable at short timescales than at the timescale of months to years measured by Weis (1994).

We emphasize that all planets of any plausible interior composition are larger than $1.5\,R_\oplus$. This comes from the mass-radius relation for cold homogeneous iron planets (Seager et al. 2006, in preparation). Iron is the densest of the abundant materials from which planets are formed. Its unlikely that a planet would be solely composed of iron, and one that was made up of any other material would be less dense and hence larger. Similarly, including temperature affects for a planet in an 0.041 AU orbit around an M star will make the planet larger; marginally so for a rocky planet, and more so for a gas planet. For reference, the terrestrial planets of the solar system have iron cores; Mercury has a 60%–70% iron core by mass, and Earth has a 32.5% iron core by mass (with 10% made up of a lighter material).

The absence of detectable transits means the radius and hence the nature of GJ 581b remains unknown. Planets larger than our detection limit of $1.48\,R_\oplus$ may include "rock giant" silicate planets, like massive Earths, a water world (akin to Neptune without a gas envelope), or even an evaporating gas planet.

REFERENCES

Baraffe, I., Chabrier, G., Allard, F., & Hauschildt, P. H. 1998, A&A, 337, 403

Baraffe, I., Chabrier, G., Barman, T. S., Selsis, F., Allard, F., & Hauschildt, P. H. 2005, A&A, 436, L47

Bonfils, X., et al. 2005, A&A, 443, L15

Butler, R. P., Vogt, S. S., Marcy, G. W., Fischer, D. A., Wright, J. T., Henry, G. W., Laughlin, G., & Lissauer, J. J. 2004, ApJ, 617, 580

Delfosse, X., Forveille, T., Mayor, M., Perrier, C., Naef, D., & Queloz, D. 1998, A&A, 338, L67

Dravins, D., Lindergren, L., & Mezey, E. 1998, PASP, 110, 610

Hamuy, M., et al. 2006, PASP, 118, 2

Hardie, R. H. 1962, in Astronomical Techniques, ed. W. A. Hiltner (Chicago: Univ. Chicago Press), 180

López-Morales, M. 2006, PASP, 118, 716

Marcy, G. W., Butler, R. P., Vogt, S. S., Fischer, D., & Lissauer, J. J. 1998, ApJ, 505, L147

Rivera, E. J., et al. 2005, ApJ, 634, 625

Rowe, J. F., et al. 2006, ApJ, 646, 1241

Weis, E. W. 1994, AJ, 107, 1135